Macromolecular Chemistry and Physics
www.mcp-journal.de

Recent Progress in Understanding Polymer Crystallization

Kay Saalwächter, Thomas Thurn-Albrecht, and Wolfgang Paul*

Dedicated to Gert Strobl and Hans-Wolfgang Spiess on the occasion of the latter's 80th birthday, honoring their important contributions to the field

Recent developments concerned with elucidating the semicrystalline structure formation in bulk polymer melts, with a focus on possibly important factors that have received less systematic attention, are reviewed. This includes the presence or absence of chain motion through the crystallites, which has a strong impact on the final crystallite thickness, and the effects of entanglements, which limit crystal growth and lower the crystallinity. From the theoretical side, interest is shown in shedding light on the thermodynamic driving forces of polymer crystallization, thus providing a theoretical background against which the kinetic limitations determine the resulting structures in experiments.

1. Introduction

From the earliest days of polymer science, the (semi)crystalline structure formation of long-chain molecules has been one of the core research topics. On the one hand, the ability of polymers to crystallize at least partially in a way that the unit cells are much smaller than the size of the macromolecule was a key question in Staudinger's debates.[1] On the other hand, and with high significance for the most common use of polymers as construction materials, the mechanical properties of a crystallizable polymer are completely dominated by the semicrystalline morphology. This holds for both the modulus in the linear regime as well as the ultimate properties, governed by the crystalline scaffold (thus the overall crystallinity) and the topology in the amorphous phase (containing tie chains and entanglements), respectively.[2]

Most of the available textbooks on polymer physics and polymer crystallization up to the present day[3–5] focus on the classical understanding of the rules governing the formation of the lamellar crystals via the famous secondary nucleation model[6] developed by Hoffman and Lauritzen (HL). This model and a number of competitors explain the selection of a specific lamellar (= crystallite) thickness on the basis of kinetic arguments, inspired by concepts from solid-state physics yet ignoring relevant polymer aspects such as topological constraints and a prediction of the degree of crystallinity. It should therefore not come as a surprise that over the years, a host of observations has accumulated that is not in agreement with the classical understanding.[7]

As a specific curiosity, we may highlight the recent work of Fritzsching and Schmidt-Rohr, who have worked out that most of the textbook pictures of lamellar crystallites are in fact wrong,[8] as they all too often show parallel stems oriented along the lamellar plane normal. For long chains with a high chain flux in the crystal such as PE such an orientation is highly unlikely in view of the resulting density anomaly, calling for chain tilt and thus more or less disordered chevron-like structures of the fold surface. Simplifying arguments, for example in terms of well-defined surface energies, appear critical in this light. Another important development concerns the question, why crystal growth in polymers leads to the formation of stacks of crystalline lamellae, whose crystal lattices are often correlated. Reiter and coworkers suggested a specific mechanism of self-induced nucleation related to a dendritic growth of the initiating lamellar crystals to explain this feature.[9]

Here, we review current work on polymer crystallization and the semicrystalline morphology covering the last decade, with a focus on a few specific yet important factors that have been underestimated and underrepresented so far, namely the role of chain entanglements and the fact that many but not all polymers exhibit diffusive chain motion through the crystals. Also, we are using a new Monte Carlo simulation approach to get a better understanding of the thermodynamic driving forces of polymer crystallization. Works along these lines have to a significant degree been pursued in a large-scale initiative funded by the German Research Foundation (DFG), namely in the framework of the Collaborative Research Centre Transregio CRC-TRR 102 "Polymers under multiple constraints." We will present some of our key results and discuss them in the context of related recent developments.

While the given topic may be considered somewhat revisionist, we would like to stress that a better understanding of polymer crystallization will help to address one of the most pressing long-term challenges in polymer science, namely the question about how we can help transforming plastics economy toward

K. Saalwächter, T. Thurn-Albrecht, W. Paul
Institute of Physics
Martin Luther University of Halle-Wittenberg
06099 Halle (Saale), Germany
E-mail: kay.saalwaechter@physik.uni-halle.de

The ORCID identification number(s) for the author(s) of this article can be found under https://doi.org/10.1002/macp.202200424

DOI: 10.1002/macp.202200424

being more sustainable.[10] The recycling of semicrystalline thermoplastics, making up the vast majority of plastics materials in use, is a good example in this regard, as the mechanical properties (in particular the ultimate properties) depend on the molecular-weight (MW) distribution (and of course possible additives), prominently trough entanglements and tie chains in the amorphous phase. Re-balancing the MW of recycled material either on the level of existing chains or just the monomers is economically most feasible for polymers with labile bonds along the main chain, for which polyesters are attracting significant current attention.[11] Especially long-chain aliphatic polyesters may have property profiles close to that of different polyethylene (PE) grades, also owing to the fact that they crystallize in a similar unit cell. Elaborating this example a bit further, thus stressing the relevance of basic polymer-physics research, it is astonishing to see that the ester groups may either form separate crystal planes (forming a larger unit cell along the crystallographic *c* direction) and thus act as structure-directing element,[12] but may also be disordered along the chains, imparting dynamics and thus opening avenues toward a larger variety of structures and properties.[13,14] Iso-dimorphism, that is the possibility of different monomers to be part of a common crystal structure, is another frequent feature of copolyesters[15] and no less important in enabling a better recycling. It should also be noted that many such materials are biodegradable. We will come back to these phenomena in the following sections.

2. Effects of Intracrystalline Chain Dynamics

The possibility that chains can move within or even through their crystals, prominently in PE, has been recognized very early on, resting on the observation of a mechanical loss peak that correlates with crystallinity.[16] In his two well-known reviews,[16,17] Boyd established the classification of crystal-mobile polymers featuring such phenomena, and crystal-fixed polymers. He pointed out a correlation with the degree of crystallinity, where typically only crystal-mobile polymers reach crystallinities in significant excess of 70%. An important related aspect known for a long time is post-growth thickening of the lamellar crystals resulting from intracrystalline chain diffusion, the most direct observation is probably represented by combined optical microscopy and AFM observations of polymer single crystals by Reiter.[18] This is naturally a slow process showing logarithmic time dependence, owing to the constraints posed by the developed crystals and in bulk by the lamellar stack. This process thus only has a small impact on the semicrystalline morphology.

With higher relevance for materials properties, Hu and Schmidt-Rohr established a connection of crystal mobility with ultradrawabilty,[19] which enables the solid-state drawing of high-strength fibers through a complete reorganization of the semicrystalline structure. They also pointed out the important role of solid-state NMR spectroscopy methods to study this process directly,[20–26] identifying individual jumps of single monomers along the helical raster of the crystalline stems, also referred to "helical jumps," as the elementary process. They are in turn mediated by fast-moving conformational defects.[27] The NMR-accessible timescale $\langle\tau_c\rangle$ is literally the average residence time of a given monomer in its raster position, as determined in most of the above works with the exception of those employing

Table 1. Timescales relevant for polymer crystallization, related to the crystallites (upper part) and to the amorphous phase (lower part).

Symbol	Definition	Meaning
$\langle\tau_c\rangle$	Helical-jump time	Average residence time of a monomer on the crystal lattice
τ_{stem}	Stem lifetime	Timescale at which displacement after many helical-jumps equals the crystallite thickness (1D random walk)
τ_{lc}	Layer crystallization time	Average time for the lateral crystal size to increase by one chain thickness
τ_d	Terminal time	Time for reptation motion by one contour length (1D random walk)
τ_{cc}	Coil crystallization time	Time for a crystal growth front to traverse a single-coil domain (end-to-end distance)
τ_e	Entanglement time	Tube-model timescale separating the Rouse from the constrained-Rouse regime
τ_{sg}	Stem growth time	Timescale of stretching of a Rouse subunit having the contour length of a crystalline stem

^{13}C-based T_1/exchange-NMR experiments.[20–22] The latter provide information on full-stem motion into the amorphous phase on a timescale of τ_{stem}, referred to as stem (life)time, see below. These timescales, as well as the ones becoming relevant further down, are summarized and explained in **Table 1**.

Along these lines, Miyoshi and coworkers documented a relation between intracrystalline dynamics and the morphology. In special cases where different crystalline forms of a given polymer could be compared, such as the polymorphic isotactic poly(1-butene)[23] or the crystalline atactic versus isotactic poly(norbornene),[26] the respective forms having intracrystalline mobility showed significantly larger lamellar thickness as well as higher crystallinity, as expected.

In an effort to establish another model polymer with high intracrystalline mobility besides PE, we studied the helical jumps in poly(ethylene oxide), PEO, in some detail.[25] PEO is advantageous in that it is readily available with controlled molecular weight (MW) and small polydispersity, allowing for systematic studies. We could establish a correlation of the average helical-jump time $\langle\tau_c\rangle$ with the crystallite thickness, which can be explained by the migrating defects' origin in the amorphous phase, such that shorter stems feature an on average higher concentration of traveling defects. This interpretation is well in line with observations from molecular simulations of PE.[27] The dilution of high-MW PEO with oligomers that preferentially remain in the amorphous phase was also found to enhance intracrystalline dynamics, on the one hand due to faster dynamics in the amorphous phase (enhancing the defect generation) and on the other hand due to somewhat thinner lamellae.[28]

Turning to mechanistic implications, in the late 1980's and still rooted in the influential HL model of secondary nucleation,[6] Hikosaka stressed the relevance of "chain-sliding diffusion"[29] within the (secondary) nucleus at the growth front. Together with Keller and coworkers,[30] a relation was established to the large lamellar thicknesses observed in poly(ethylene) crystallized under high pressure, which occurs through the highly mobile hexagonal rotator phase following Ostwald's rule of stages. These

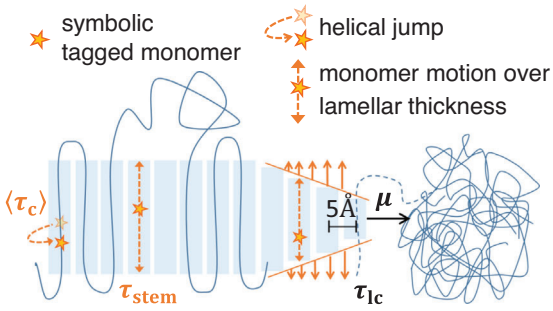

Figure 1. Mobility of polymer stems on a timescale τ_{stem} through a given lamella, arising from traveling defects leading to helical jumps of the monomers with correlation time $\langle\tau_c\rangle$, enables lamellar thickening directly at the advancing growth front.[32,33] This timescale, as compared to the attachment time of a single-chain layer (τ_{lc}) derived from the lamellar growth velocity μ, turns out to be a relevant morphological control parameter. Reproduced under the terms of the CC BY 4.0 license.[34] Copyright 2022, The Authors. Published by Springer Nature.

ideas, along with extensive experimental investigations of lamellar thickness upon crystallization and melting, led Strobl to formulate a general multi-stage model of polymer crystallization.[31] Consequentially, it's main assumption to explain the lamellar thickness moves away from the kinetic-selection arguments of HL but rather relies on considerations of (local) thermodynamic stability.

Taking up Hikosaka's idea of sliding diffusion at the growth front (see **Figure 1**), Hu and coworkers suggested that the sliding diffusion may be responsible for an on-growth thickening,[32] which offers an alternative explanation of Strobl's crystallization and melting lines, which were the basis of his multi-stage model.[31] Since this work was based upon highly coarse-grained computer simulations, the extrapolation of the timescales of chain diffusion and lamellar growth to actual experimental conditions remained uncertain.

In our work, we decided to address the problem systematically, by comparing isothermally crystallized polymers with defined and narrow MW distribution and with well-characterized but different intracrystalline chain dynamics. In a first step, we focused on the detailed semicrystalline morphology as obtained from SAXS studies. Importantly, we rely on a novel approach of data analysis based on a specific model of the interface distribution function (IDF), implementing a paracrystalline layer model allowing for distributions of the crystallite and amorphous thicknesses (d_c and d_a, resp.). The model thus provides two more relevant parameters, namely the standard deviations $\sigma_{a,c}$ of these two quantities.[35] Typical results of such analyses are shown at the left hand side of **Figure 2**A for two model polymers, namely poly(ϵ-caprolactone), PCL, and PEO.

While PCL was earlier shown to be crystal-fixed,[36] meaning that a combination of NMR methods suggested the absence of helical jumps faster than about 1 s, PEO features rather fast intracrystalline mobility at typical temperatures of crystallization.[25] Rather simple ^{1}H low-resolution NMR methods, namely temperature-dependent free-induction decays (FIDs) are actually suited to extract the helical jump time $\langle\tau_c\rangle$, as shown in the middle panel of Figure 2A. In our comparative work,[33] polarized optical microscopy was further applied to measure the speed of the lamellar growth front μ, from which the layer crystallization time τ_{lc} can be derived, see Figure 1. For PEO, this time turns out to be comparable to the time it takes for a given monomer to diffuse over the length of a whole stem τ_{stem} (the lifetime of a stem). As discussed above, the latter is only available from a specific yet simple 1D diffusion model taking $\langle\tau_c\rangle$, which is the NMR-based residence time of a monomer in a given raster, as the elementary step. This includes the assumption of unrestricted back-and-forth motions, which may not be fully justified in all cases,[20–22] meaning that our τ_{stem} represents a lower (fast-end) limit. Nevertheless, we could thus provide for a first time an experimental justification of the wedge-shaped grown front depicted in Figures 1 and 2A (right bottom part).

The main body of results from this work is shown in Figure 2B.[33] In these plots showing the relevant dimensions of the lamellar stacks as a function of isothermal crystallization temperature, the "error bars" quantify the fitted width $\sigma_{a,c}$ of the layer-thickness distributions. The notable observations are that in the crystal-mobile case (PEO), the amorphous thickness d_a is rather well-defined, while in the crystal-fixed case (PCL), d_a has a wide distribution, as opposed to a very well-defined crystallite thickness d_c. Our interpretation was that the on-growth thickening in PEO allows for a maximization of d_c, thus establishing a minimal and defined d_a that is governed by the remaining entanglements. The role of entanglements is taken up in the next section. In contrast, without on-growth thickening, d_c of PCL is the well-defined quantity, arising from the initial kinetic or local-thermodynamic selection.[37]

We note that these results are not in agreement with earlier conclusions based upon a related approach by Stribeck and Zachmann,[38,39] who were the first to derive distribution information by fitting of the SAXS-based IDF. They noted that "*in previous studies it was found that the relative width of the distribution of the crystallite thicknesses is, in general, the narrower one*"[39] and concluded this to be a possible means to distinguish the crystalline from the amorphous layer spacing (we do this by observing the systematic changes upon melting and by comparison with alternative means to measure the crystallinity, namely NMR). Our approach may be the more robust choice, fitting directly in reciprocal space (avoiding the intermediate Fourier transform) and thus considering all contributions to the IDF (and not just the first three contributions) together with a reliable determination of the Porod constant. Moreover, Stribeck and Zachmann studied their samples at room temperature. We know that additional crystallization during cooling after isothermal crystallization takes place in different ways in the crystal-mobile and crystal-fixed cases, showing thickening versus insertion, respectively. A direct comparison of their results with ours is thus encumbered. Our general conclusions have in fact been confirmed independently by Toda[40] applying a different yet related fitting approach to a pair of a crystal-fixed polyester (PBT) and the crystal-mobile PE.

An independent confirmation of the relevance of on-growth thickening is provided by SAXS[33] and fast-scanning-DSC studies[37] of the reorganization in PEO versus PCL on heating. In PEO, melting of the already thickened and thus stabilized lamellae occurs at a defined melting point T_m. This is in significant contrast to what happens on heating of PCL, which undergoes continuous melting and recrystallization, simply because the comparably thin crystals, formed at T_c and not

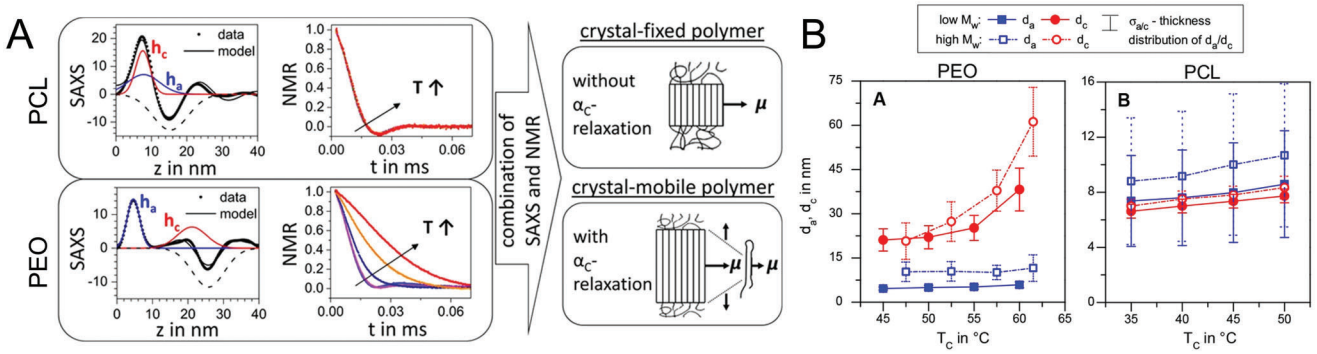

Figure 2. A) Combined SAXS-NMR approach establishing morphological differences and classifying PCL and PEO as crystal-fixed and crystal-mobile polymers, respectively. The SAXS-based interface distribution function (left) reveals the distribution width of the domain thicknesses shown in (B), while the NMR-based free-induction decays reflect fast chain mobility in terms of a temperature-dependent transverse relaxation time. Reproduced with permission.[33] Copyright 2018, American Chemical Society.

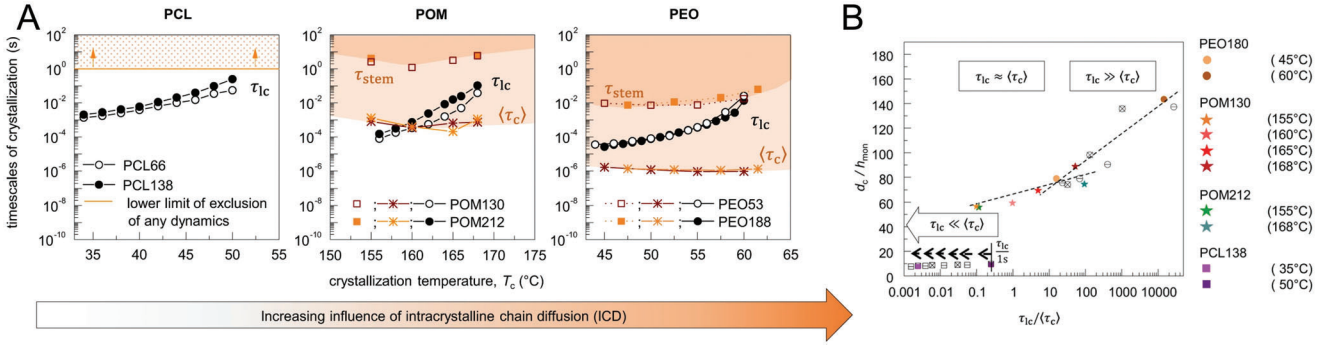

Figure 3. A) Timescales relevant for lamellar growth (see Figure 1) for PCL, POM and PEO for different isothermal crystallization temperatures. B) Normalized crystallite thickness (in units of monomers per stem) as a function of the ratio of the layer crystallization time and the helical jump time. Reproduced under the terms of the CC BY 4.0 license.[34] Copyright 2022, The Authors. Published by Springer Nature.

thickened/stabilized, also melt at nearly the same temperature and immediately re-form on further heating with increased d_c.

To support our findings on a broader basis, and in the attempt to establish a quantitative relationship between crystallite thickness and on-growth thickening, we included a third polymer into our comparisons, namely polyoxymethylene, POM.[34] This polymer shows comparably slow helical jumps as quantified by more advanced solid-state NMR methods adapted to slower motions, and thus represents a suitable in-between case. This is depicted in **Figure 3**A showing the relevant crystallization timescales. The layer crystallization time τ_{lc} always has the strongest T_c dependence in all cases, and is of the order of the helical-jump time in POM. This is in contrast to PEO, where it actually reaches the stem exchange time at relevant T_c.

With all timescales known, we could thus attempt a correlation of the normalized crystallite thickness of all these polymers with the ratio $\tau_{lc}/\langle\tau_c\rangle$ quantifying the importance of chain diffusion versus growth velocity. The plot in Figure 3B shows a rather clear correlation extending over various samples at significantly different T_c. Note that the data for PCL seem to not match the trend only because we arbitrarily set $\langle\tau_{lc}\rangle$ to the minimum value of 1 s marking our detection limit. The correlation shows a clear indication for a regime change when τ_{lc} and $\langle\tau_{lc}\rangle$ (and with it τ_{stem}) are of comparable magnitude. With all of this, we claim to have made the first step toward a more general quantitative understanding of the mechanism of selecting the crystalline thickness, which for crystal-mobile polymers is obviously much larger than the initial value.

In the Introduction, we have stressed the growing importance of aliphatic polyester-based semicrystalline thermoplasts as potentially more sustainable, recycling-friendly alternative to PE with similar properties.[11] Aliphatic polyesters (such as PCL) feature essentially the same orthorhombic unit cell as PE, but with a much larger *c* spacing, accommodating the ester groups in layers. As a result, helical/monomer jumps are unfavorable, rendering such materials crystal-fixed,[19] thus imparting limitations with regards to maximizing the crystallinity upon processing. However, as the example shows, the PE unit cell is able to accommodate quite a variety of "chemical defects" such as the ester group or simpler ones such as C=O or pending methyl groups or halogens. Such defects can also be present in an irregular fashion without forming layers, and notably, the materials can then exhibit an intracrystalline relaxation detectable by, for example, mechanical spectroscopy. An interesting example[13] are linear aliphatic co-polyesters made from caprolactone and pentadecalactone, P(CL-*co*-DL). Recently, a layered–unlayered crystal transition was observed even in regular long-spaced aliphatic polyesters,[14] and attributed to the possibility of intracrystalline

chain motion in the unlayered form. Therefore, future work should focus on processing conditions where crystal mobility in special polymorphic forms could be harnessed to tune the semicrystalline morphology and thus optimize the materials for their intended application. This also includes the potential to modify the entangled structure, which we now turn to.

3. Entanglement Effects

As noted in the Introduction, entanglements residing in the amorphous phase are a key feature governing the mechanical properties of semicrystalline polymers in particular at large deformations.[2] The question how entanglements interfere with semicrystalline structure formation, in particular whether a "reeling-in" process may help with speeding up and thus enabling distantanglement at the growth front of high-MW polymers, has been the subject of the famous 1979 Faraday Discussion of the Chemical Society.[41] The discussion was partially spawned by an earlier review article of Flory and Yoon, who argued against adjacent-reentry structures in bulk polymer crystals on the basis of a general unlikelihood of the necessary disentanglement, and concluded that entanglements are mostly preserved and concentrated in the amorphous phase.[42] A final consensus was beyond reach in those days. According to Hikosaka, sliding diffusion could be a relevant process, not considered in the earlier discussions, to explain local and global disentanglement.[43] However, evidence for the argument was mainly taken from observations of primary nucleation and thus restricted to early-stage processes.

Entanglement effects on polymer crystallization are naturally studied via attempts to modify the entanglement density under crystallization conditions. This is beset with conceptual difficulties, as changes of the system are often rather non-trivial and do not readily reflect the conditions of crystallization in bulk, as it is relevant in processing of thermoplastics. The study of crystallization from dilute solutions is a natural choice to avoid entanglement effects altogether, but leads to very special structures (often single crystals) that are not comparable to the lamellar-stack structure formed in the bulk.[44] Single- or few-chain crystals are also available from catalytic PE syntheses ("reactor powder"), and melting such crystals results in non-equilibrium disentangled melts, the crystallization of which can then be studied.[45] Freeze-drying of dilute solutions is another means to achieve a similar starting situation.[46]

One complication is that the re-entanglement of such non-equilibrium melts occurs surprisingly fast (i.e., on timescales shorter than terminal relaxation of the homogeneous melt).[47] This was very recently also illustrated in a comparative NMR-study of solution- versus bulk-crystallized high-MW PE.[48] Moreover, most works along these lines often focused on kinetic aspects (primary nucleation, bulk crystallization rate, etc.), yet crystallization from such larger-scale heterogeneous states will always have a significant impact on the final morphology that is not easily separated from the actual effect of entanglement density. There is little doubt that entanglements limit the growth of the crystalline phase,[49] but consequently, surprisingly little attention was paid to the interplay of entanglements and the bulk morphology, in particular to the actual size of the amorphous phase (d_a).

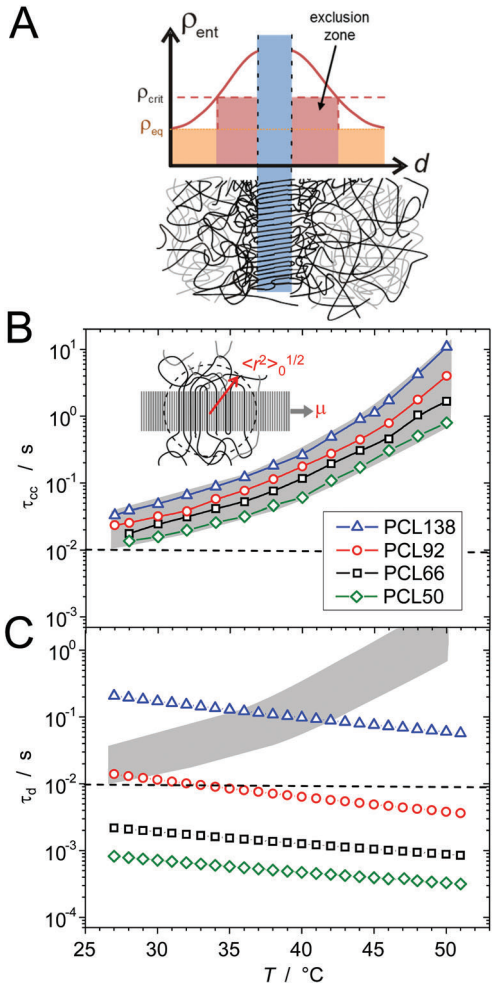

Figure 4. A) Model explaining a limitation of crystallinity via an exclusion zone with enhanced entanglement density around a given lamellar. B) Coil crystallization time of various PCL samples derived from the lamellar growth velocity measured in polarized optical microscopy, and C) terminal time of the same samples measured by melt rheology, both as a function of temperature. The identical shaded area in both plots provides a comparison. Reproduced with permission.[52] Copyright 2018, American Chemical Society.

One prominent exception and the starting point of our own investigations is the work of Jacques Rault,[50] who was probably the first to provide evidence for the claim that unresolved entanglements govern d_a and thus limit the crystallinity. This scenario is depicted in **Figure 4**A, where a region of increased entanglement density acts as an exclusion zone for further crystallization by "entropic repulsion," mostly through excluding additional lamellae to approach the given one. There seems to be only one, although little recognized effort by Iwata to cast this idea into a theory.[51] Rault suggested that one should compare two new timescales separating the regimes of slow and fast crystallization, with regards to the ability of the chains to disentangle via reptation in the quiescent melt or not, respectively. Disentanglement is quantified by the terminal time τ_d, which in "slow crystallization" would be shorter than the time it takes for an advancing lamella to grow through the region occupied by the given polymer coil.

As depicted in the inset of Figure 4B, the related "coil crystallization time" τ_{cc} is again available from the lamellar growth velocity μ observed in polarized optical microscopy in combination with the known end-to-end distance in the melt.

Figure 4B,C shows data from our attempt to study polymer crystallization in the bulk across this regime transition, using well-entangled, crystal-fixed PCL over a large MW range from about 50 kDa up to millions.[52] We measured the lamellar growth velocities and derived τ_{cc}, and performed shear rheology to extract τ_d, both shown as a function of crystallization temperature T_c in parts B and C, respectively, As it is obvious from the shaded area in C representing the range of τ_{cc} from part B, our range of samples well covered the regimes of slow crystallization (at low MW) to fast crystallization. Interestingly, d_c of around 8 nm hardly varied across our sample series, while d_a increased from around 6 to 14 nm, with only a weak tendency toward a weaker MW dependence in the fast-crystallization regime at high MW. All in all, the crystallinity thus decreased from about 60% at the lowest MW to less than 35% at the high-MW end.

Our main aim was actually to quantify the entanglement density in the amorphous phase of these samples, so as to find possible evidence for disentanglement versus retention/accumulation. One approach to achieve this goal is to analyze the large-strain behavior in tensile[53] or compression experiments.[2] Some preliminary results concerning the former were included in our work,[52] while more detailed analyses based on the more robust compression tests are ongoing. For a direct and systematic insight into the amorphous phase of quiescent samples, we then employed a special ^{1}H NMR technique termed multiple-quantum NMR,[54,55] which is suitably applied in simple low-field low-resolution instruments.

MQ NMR probes the incomplete averaging of dipole-dipole couplings among the protons. In an isotropic liquid, this orientation-dependent spin interaction is quickly time-averaged to zero, while in cases of slightly anisotropic segmental motions induced by the presence of chain-end fixation through entanglements or crystal anchoring points, a finite measurable residual dipolar coupling (RDC) remains. This quantity is a function of temperature and experimental (pulse-sequence) time since it maps out the regimes of chain motion prescribed by the tube model of entangled polymer dynamics.[56] The (t, T)-dependence of the RDC is best described by the segmental dipolar (tensorial second-order) orientation autocorrelation function $C(t, T)$ depicted in **Figure 5**A, which roughly speaking is proportional to the square of the RDC. It is not a coincidence that this function resembles the stress relaxation modulus $G(t)$; the quantities are in fact related since flow in polymer melts is generally related to the decorrelation of segmental orientation.[56] In an entangled melt (green line), the glassy (0) and Rouse (I) regimes are followed by the local-reptation (or constrained-Rouse) regime II, which corresponds to the rubbery plateau in $G(t)$. In regimes III (reptation) and IV (flow), $C(t)$ gradually decreases and approaches zero for a bulk melt, and is delayed or even approaches a finite network-like plateau in the case of chains constrained to the amorphous region.

The complication that we had to solve is that the entanglement density is reflected by the amplitude of $C(t)$ only at the rather short entanglement time $t = \tau_e$, which is too short to reach on the ms timescale of MQ NMR (see the red question mark vs the green shaded region in Figure 5A). Simply cooling was not an option, as our samples would be compromised by additional insertion-mode crystallization. We thus had to quantify the power-law exponent of $C(t)$ in the dynamic regimes II and III, and back-extrapolate to $C(\tau_e)$. In this way, we could obtain an estimate of the increase in entanglement density of the amorphous phase of our samples as compared to the value in the bulk melt.

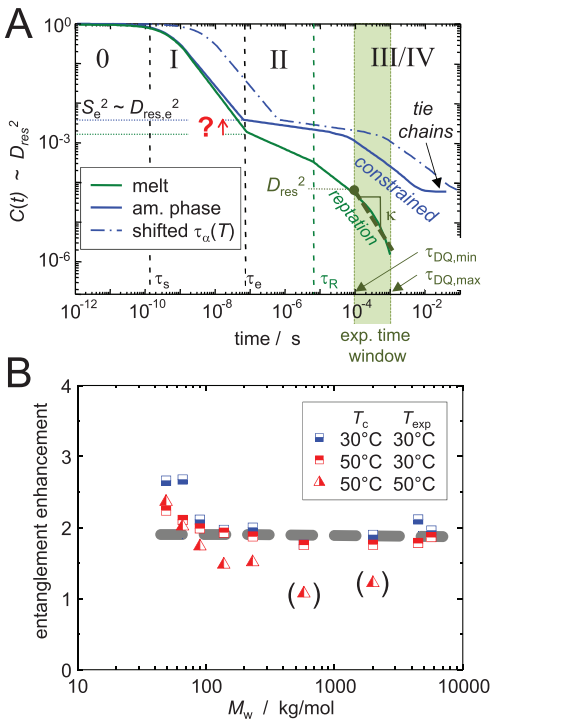

Figure 5. A) Principle of the NMR-based measurement of the entanglement density via the segmental orientation autocorrelation function, back-extrapolated to the entanglement time τ_e. B) NMR-based estimated entanglement enhancement factor for a wide series of PCL with different MW at different temperatures. Reproduced with permission.[52] Copyright 2018, American Chemical Society.

The resulting enhancement factor is plotted in Figure 5B for all samples crystallized and measured at different temperatures. Despite some variation, we could conclude that the entanglement density is on average increased by a factor of two during the crystallization of PCL. Importantly, a crosslink-like contribution of tie chains can be excluded on the basis of the comparably large dimension of d_a, being much larger than the tube diameter. We remind that the crystallinity of most of the samples was in the range of 40–60%. So with on average 50% of crystallinity, an increase in entanglement density by a factor of 2 can straightforwardly be explained by the complete retention of all entanglements existing prior to crystallization. This is strong evidence of the absence of a "reeling-in" process in our sample range. Notably, this also holds for the "slow-crystallization" regime below an MW of about 200 kDa, where the slight increase may be attributed to the influence of tie chains in the narrower amorphous layers.

We consider our findings the first objective estimate of the entanglement density in a given bulk quiescent semicrystalline polymer. The lack of finding evidence for the slow-fast

crystallization regime transition may be attributed to the fact that in the given case of a crystal-fixed polymer, terminal relaxation is effectively halted when only a single stem becomes part of the crystal. In other words, even with a small fraction of segments fixed in the growing crystal, free reptation becomes impossible and arm-retraction dynamics may just be too slow to effectively resolve entanglements.

We shall now contrast our findings with some other recent works focusing on entanglements in bulk polymer crystallization. In a series of papers, Luo and Sommer used coarse-grained molecular-dynamics (MD) simulations in combination with primitive-path analyses to study the relations between crystal nucleation and growth and the entangled state of the melt.[57–60] They found rather clear indications of a relation between the crystallite thickness and the entanglement spacing, most clearly in a system where entanglements were diluted by a short-chain solvent.[59] This is actually in line with experimental findings of Miyoshi and coworkers,[61] who have established a special solid-state NMR technique probing proximities between ^{13}C-labeled chains in the crystals to estimate the folding number of the chains. They found a similar folding number n (average number of adjacent re-entries) of order three as in the computer simulations, suggesting that a long chain can only fold locally between two entanglement points, where the folding number simply arises from the contour length of the chain between two entanglements as compared to the crystalline stem length. The finding was recently reinforced by a similar observation on samples cold-crystallized from the glassy state, where large-scale chain motion is impossible.[62] The authors concluded that folding occurs prior to crystallization within "existing templates", that is at a length scale at or even below entanglements.

Notably, Luo and Sommer found that the entanglement density actually decreased (weakly) upon non-isothermal crystallization, in some contrast to our results. However, this may be attributed to the fact the course-grained computer model allows for rapid sliding diffusion—which was not quantified. In a more recent work of Lame and coworkers, disentanglement upon crystallization was again observed by coarse-grained MD simulations, now during isothermal crystallization.[63] Notably, "sliding" diffusion was explicitly detected and concluded to be relevant. In this way, the old debate initiated by Flory and Yoon mentioned above could be partially resolved, now stating that the presence of intracrystalline chain diffusion may indeed lead to disentanglement during crystallization.

Experimentally, the groups of Men and Litvinov have very recently joined forces to compare samples of semicrystalline poly(1-butene), which can be crystallized at high temperatures in a conformationally disordered (CONDIS) phase II with high chain-sliding mobility, and then be transformed to the stable phase I via a solid–solid transition upon cooling.[64,65] Such samples can then be prepared at different isothermal crystallization temperatures, where slow crystallization at high temperature leads to thicker crystals, possibly arising from more significant disentanglement.

These authors actually employed a comparably simple ^{1}H NMR transverse-relaxometry approach to assess the entanglement density, also used before in their re-entanglement study of molten single crystals mentioned above.[48] This approach neglects the back-extrapolation to τ_e, but rather relies on acquiring data rapidly during an isothermal melting run. The entanglement density is obtained as value extrapolated to zero crystallinity (assuming that over the measured data range sufficient crystallites remain to suppress reptation and disentanglement). This means that one only has an indirect and qualitative view on the entanglements that existed in the amorphous phase. Nevertheless, the melting run of the samples prepared via the CONDIS route with different crystallization rates and for different molecular weights did show significant changes reflecting a reduced entanglement density, providing evidence for disentanglement during crystallization in the presence of fast intracrystalline mobility. In our group, we are currently trying to probe disentanglement during crystallization in the simpler case of crystal-mobile PEO, which does not exhibit and should not require such a polymorphism.

Finally, very recent work from our group was focused on a quantitative assessment of the relation between the entanglement density of a bulk melt and the resulting amorphous-phase thickness. This work is still to be published, but a preprint is available online.[66] A feasible way to control the entanglement density is the use of low-molecular additives, for example simply solvents.[67] While avoiding the above-mentioned complications related to heterogeneous non-equilibrium structures, thermodynamic effects, that is melting point depression and phase separation induced by crystallization, then come into play. To avoid these, we have designed a bimodal blend system of high-MW PCL with an oligomeric PCL as diluent that: i) happens to exhibit the same crystallite thickness as the high-MW component and consequently; ii) forms co-crystals when the study is performed at sufficiently fast crystallization (high supercooling).

The entanglement density of the melts prior to crystallization was quantified by shear rheology, and could be quantitatively related to the measured amorphous thickness over a wide range of polymer-oligomer mixtures. The results are compatible with an attractively simple model without adjustable parameters, based upon the justified assumption that disentanglement is negligible in the crystal-fixed case, for reasons discussed above. Together with the result introduced above, where we showed that the crystallite thickness in PCL after isothermal crystallization corresponds to the minimum thickness required for thermal stability, we thus achieved here for the first time a full empirical understanding of the structural parameters of the semicrystalline morphology, including an important parameter having received little attention, namely the overall crystallinity.

4. New Theoretical Insights

All experimental findings on polymer crystallization from the melt establish without doubt, that the semi-crystalline morphology of polymer materials is a kinetically arrested non-equilibrium structure. As discussed above, the general theoretical approach for the description of polymer crystallization since the times of HL[6] assumes a kind of equilibrium (or at least meta-stable equilibrium) approach, using thermodynamical concepts like free energies. But one can approach the process of lamella formation in polymer crystallization from a different point of view, focusing on a kinetic picture[68] instead. The relevance of the ratio of the time scales inherent to crystallite growth to the relaxation time scales

of the chains in the amorphous region was pointed out long ago by Flory and Yoon.[42]

Crystallization is driven by packing constraints of excluded volume. In crystallizing polymers, this typically goes hand in hand with an intramolecular stiffening of the chains. So for a new stem to attach to a growing crystal a certain length of chain has to rearrange its conformation from the amorphous melt state to the stretched out stem state. For the average time, τ_{sg}, to grow a stem of length d_l (in number of segments) one can formulate a phenomenological ansatz $\tau_{sg} = d_l/(v_0 + c\Delta T)$. Here, $\Delta T = T_c^0 - T$ is the super-cooling, the phenomenological factor c translates this supercooling into a growth velocity, and v_0 is a contribution to the growth velocity taking into account the driving force due to the vicinity of a crystallite surface. This relaxation process occurs on the time scale of the Rouse time of a part of the chain with the same contour length as the stem. Equating the stem growth time with the Rouse time of a chain segment of the same length at the melting temperature one obtains

$$d_l(T) = \frac{3\pi^2 k_B T_m^0}{\zeta c (T_c^0 - T)} \quad (1)$$

where ζ is the monomeric friction in the amorphous phase and $T_c^0 = T_m^0 + v_0/c$. This simple phenomenological ansatz reproduces the experimental difference between crystallization and melting line and their dependence on the lamellar thickness found in some experiments,[7] although recent experiments obtained with the new technique of fast-scanning-DSC put these results into question.[37]

One central idea about the driving force for polymer crystallization within this argument is a well-known result from equilibrium statistical mechanics: crystallization is governed by excluded-volume interactions. Even the most simple model liquid, a dense system of hard spheres, completely crystallizes beyond a volume fraction of $\phi = 0.545$[69] to maximize translational entropy. Of course, the hard-sphere idea is a theoretical idealization which can as such only be realized in a computer simulation, but some model colloid systems follow this prediction very well.

For polymer crystallization the situation is more complex, as it goes along with conformational and orientational ordering in addition to positional ordering. To understand the thermodynamic driving force in this case in a computer simulation study, one has to avoid the kinetic arrest and be able to determine the thermodynamic equilibrium over a wide temperature range. There is a long and successful tradition of MD simulation studies of polymer crystallization which have helped to understand, for example, the importance of entanglements on the crystallization[57–60,70] or the molecular processes underlying nucleation and growth of crystal lamella.[71,72] However, the MD technique is not able to address the equilibrium behavior of these crystallizable polymer models. This can be done by studying a hard-sphere chain model where a bending potential increases the chain stiffness upon cooling.[73,74] Such chain stiffening is also central for the crystallization in experiments. Conformational and orientational ordering induces lamellar structure formation which is observable as a small angle scattering peak (SAXS), whereas the local positional ordering gives rise to a wide angle peak (WAXS). Experimentally, they occur almost simultaneously upon super-cooling a polymer melt.[75] But which of the two ordering processes drives the crystallization?

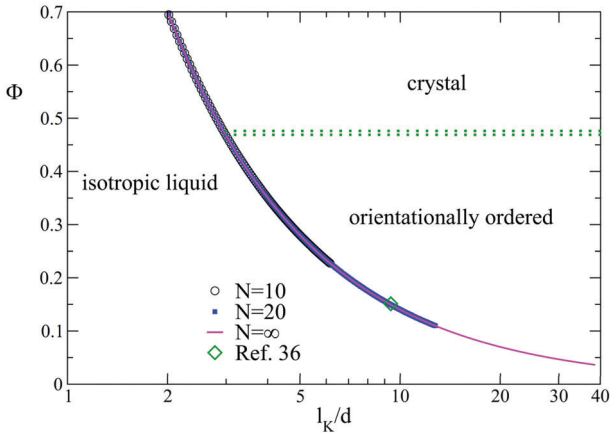

Figure 6. Phase diagram of a crystallizable polymer in the stiffness-volume fraction plane. Stiffness is encoded in the aspect ratio $l_K(T)/d$, Kuhn length over chain thickness, typical for the Onsager theory of orientational ordering. Data points are the aspect ratios realizable for the two chain lengths, the magenta line is a phenomenological fit. The green region is the coexistence region between a 2D disordered state perpendicular to the chain backbones and the crystal state. Adapted with permission.[73] Copyright 2018, American Physical Society.

We addressed this question by simulations of semi-flexible hard-sphere chains of length $N = 10$ and 20 using an advanced flat-histogram Monte-Carlo technique.[76,77] These chains are long enough to follow Rouse dynamics and display Gaussian conformations in the melt where they are still flexible. The equilibrium phase diagram of this model suggests the following picture (**Figure 6**). One knows that a dense system of flexible hard-sphere chains of length $N = 12$ becomes completely crystalline at a volume fraction $\phi \approx 0.56$,[78] which is larger than for the hard-sphere liquid, because the translational entropy of a chain of length N is reduced by a factor $1/N$ compared to the simple liquid. However, we find that a sufficiently stiff hard-sphere chain already crystallizes at $\phi = 0.47$. So it is the Onsager-type orientational ordering between stiff chains that drives the crystallization process (SAXS). The magenta line in Figure 6 is the Onsager prediction separating the isotropic from the nematic states. In the simulations this orientational ordering occurs simultaneously with a positional ordering on the repeat unit scale (WAXS) if the areal density perpendicular to the stems in the lamellae is large enough (above the green coexistence region in Figure 6). For smaller volume fractions, the phase diagram predicts the possibility of nematically ordered semi-dilute phases, which have also been experimentally observed.[79] We thus established orientational interactions as the thermodynamic driving force of polymer crystallization for relatively short chains. However, from our general understanding of the statistical thermodynamcis of polymers, no new possible driving forces arise when we increase the chain length. So we conjecture that our picture also holds for melt crystallization of long chains, but this remains to be tested experimentally.

It is a specialty of polymers that even a single chain can be a thermodynamic system in its own right undergoing phase transitions like crystallization when the chain length diverges. Such

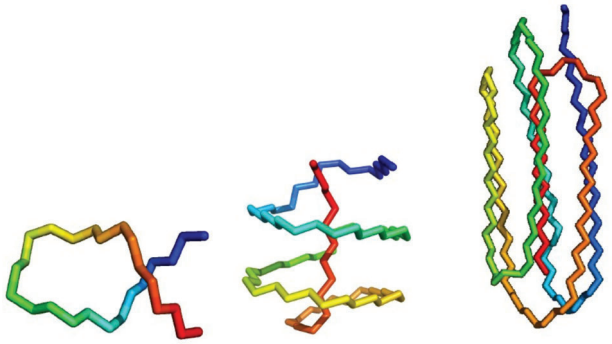

Figure 7. Snapshots of ground-state structures for single alkanes of different lengths: $N = 28$ on the left folds into a twisted hairpin structure, $N = 60$ in the middle into a filled helical structure, and $N = 150$ on the right forms the lamella crystal typical for polyethylene. The color code runs from one chain end to the other.

single-chain transitions can by studied with the above mentioned method even for a chemically realistic model of polyethylene. On finds that one needs a minimum chain length of about $N = 150$ for the lamellar crystal to be the thermodynamic ground state[80] of a single chain (**Figure 7** right). The lamellar thickness of these is smaller than would be the case for melt-crystallized chains of the same length. For shorter chains one interestingly observes ordering types which are reminiscent of the secondary and tertiary structures of proteins, like hairpins (Figure 7 left) or filled helices (Figure 7, middle). Such ordering is thus revealed as being a consequence of stiffness and packing constraints introduced by chain collapse induced by attractive interactions.

While it is intriguing to find protein-like secondary structures even for the most simple synthetic polymer, one has to be aware of significant differences due to the lack of strong specific interactions in the alkanes. In proteins, hydrogen bonds not only lead to a much higher ordering temperature but also to structural differences, like flat β-sheets and unfilled α-helices, which are not favored by the isotropic van der Waals interaction of the alkanes. A 1D aggregation process, as it occurs in the amyloid formation of proteins based on β-sheet stacking, is typically not realized for synthetic polymers. However, given the ubiquity of amlyoid fibril formation for a broad range of protein primary sequences, a careful design of a synthetic heteropolymer including hydrogen bonding units should be able to introduce such 1D aggregation from solution also into the world of synthetic polymers. A quasi-1D crystal growth stabilized through specific interactions has been found for poly-3-hexylthiophene,[81] where the easy direction of growth is given by the π-stacking direction of the thiophene rings.

5. Conclusions

This perspective reported on a series of experimental and theoretical results on polymer crystallization obtained during the running time of the Collaborative Research Centre SFB TRR 102. Experimentally, the determining kinetic factors for the semicrystalline morphology resulting from isothermal polymer crystallization were clearly established in a combined SAXS and NMR approach. We could show that a whole range of dynamic processes and their differing temperature dependencies interact to determine the degree of crystallization achievable and the size distributions of crystalline and amorphous domains that are formed.

These processes range from the timescale for defect/monomer motion within the crystal lamellae via the attachment time of a single-chain layer, the time for stem motion up to the disentanglement time in the amorphous layers. The first three are decisive in determining the size distribution of crystalline and amorphous regions in the semi-crystalline material. When the timescale for monomer motion is much larger than the one for single-layer attachment, one has a crystal-fixed polymer and for these, the thickness of the amorphous regions shows a broad distribution while the crystallite thickness is rather well-defined. The opposite behavior is observed for the crystal-mobile case, where the monomer motion is faster or comparable to the layer attachment timescale.

The large-scale motion in the amorphous phase with its disentanglement timescale seems to loose its significance for high-MW crystal-fixed polymers, where fixation of a train of monomers in a stem halts terminal dynamics and the number of entanglements seems to be conserved in this case, which leads to an increase of entanglement density in the amorphous regions. This in turn sets a lower bound for the size of these regions and thereby an upper bound for the crystallinity that can be reached. Future work should clarify the significance of chain motion through the crystals in the crystal-mobile case, which could still allow for terminal relaxation and thus significant disentanglement and the resulting in increase in lamellar thickness and crystallinity. First experimental results for special cases and also computer simulations point into this direction.

The theoretical work performed was complementary to the experimental efforts. Polymer crystallization is a phase transition that is kinetically limited by the processes studied in the experiment. Experimentally it was well known that the large- scale structure formation (lamellar scale) and the local positional ordering (atomic scale) seem to occur concurrently, but it was unclear which of the ordering processes drives the crystallization in polymers. Studying a simplified model which nevertheless captured the important ingredient of chain stiffening upon crystallization, it could be established that it is the conformational and orientational ordering that drives polymer crystallization.

Finally, studying single-chain ordering of synthetic alkanes, it could be established that for chain lengths smaller than a certain threshold beyond which lamellar ordering sets in, the low-temperature states can be classified in the language of secondary and tertiary structure formation that we normally use for proteins. This establishes the possibility for a connection to aggregation phenomena in solution, especially amyloid formation, observed in many proteins.

Acknowledgements

The authors thank the Deutsche Forschungsgemeinschaft (DFG) for a total of 12 years of financial support in the framework of the SFB-TRR 102 (project-ID 189853844), projects A1 (K.S. and T.T.-A.) and A07 (W.P.). The authors are indebted to the committed undergraduate and doctoral students, postdocs as well as co-PIs having worked on their projects over the years, namely Ruth Bärenwald, Mohd Afiq Bin Anuar, Ricardo Kurz,

Tonghua Liu, Albrecht Petzold, Yu Qiang, Mareen Schäfer, Kerstin Schäler, Martha Schulz, Anne Seidlitz, Timur Shakirov, Semjon Stepanov, Niklas Wallstein, and Zefan Wang. K.S., T.T.-A., and W.P. are grateful for having been able to stand on the shoulders of their long-year mentors Hans-Wolfgang Spiess, Gert Strobl, and Kurt Binder, respectively, without whom this work would not have come into existence.

Open access funding enabled and organized by Projekt DEAL.

Conflict of Interest

The authors declare no conflict of interest.

Keywords

crystalline alpha relaxation, entanglements, helical jumps, histogram Monte–Carlo simulations, rheology, small-angle X-ray scattering, solid-state NMR spectroscopy

Received: November 23, 2022
Revised: January 20, 2023
Published online: February 20, 2023

[1] H. Staudinger, *Naturwissenschaften* **1934**, *22*, 65.
[2] Z. Bartczak, *Polimery* **2017**, *62*, 787.
[3] B. Wunderlich, *Macromolecular Physics, Crystal Nucleation, Growth, Annealing*, Vol. *2*, Academic Press, New York **1976**.
[4] U. Gedde, *Polymer Physics*, Kluwer Academic Publishers, Dordrecht **1995**.
[5] L. Mandelkern, *Crystallization of Polymers*, 2nd ed., Vol. *2*, Cambridge University Press, Cambridge **2004**.
[6] J. D. Hoffman, G. T. Davis, J. I. Lauritzen Jr., in *Treatise on Solid State Chemistry*, (Ed: N. B. Hannay), Plenum Press, New York **1976**, pp. 497–613, Ch. 7.
[7] G. Strobl, *Rev. Mod. Phys.* **2009**, *81*, 1287.
[8] K. J. Fritzsching, K. Mao, K. Schmidt-Rohr, *Macromolecules* **2017**, *50*, 1521.
[9] S. Majumder, P. Poudel, H. Zhang, J. Xu, G. Reiter, *Polym. Int.* **2020**, *69*, 1058.
[10] K. Saalwächter, *Front. Soft Matter* **2022**, *2*, 1037349.
[11] M. Häußler, M. Eck, D. Rothauer, S. Mecking, *Nature* **2021**, *590*, 423.
[12] S. F. Marxsen, D. Song, X. Zhang, I. Flores, J. Fernández, J. R. Sarasua, A. J. Müller, R. G. Alamo, *Macromolecules* **2022**, *55*, 3958.
[13] M. P. F. Pepels, L. E. Govaert, R. Duchateau, *Macromolecules* **2015**, *48*, 5845.
[14] S. F. Marxsen, M. Häußler, S. Mecking, R. Alamo, *ACS Appl. Polym. Mater.* **2021**, *14*, 5243.
[15] M. Schäfer, S. Yuan, A. Petzold, R. A. Pérez-Camargo, A. J. Müller, T. Thurn-Albrecht, K. Saalwächter, K. Schmidt-Rohr, *Macromolecules* **2021**, *54*, 835.
[16] R. H. Boyd, *Polymer* **1985**, *26*, 323.
[17] R. H. Boyd, *Polymer* **1985**, *26*, 1123.
[18] G. Reiter, *Chem. Soc. Rev.* **2014**, *43*, 2055.
[19] W.-G. Hu, K. Schmidt-Rohr, *Acta Polym.* **1999**, *50*, 3271.
[20] K. Schmidt-Rohr, H. W. Spiess, *Multidimensional Solid-State NMR and Polymers*, Academic Press, London **1994**.
[21] Y. F. Yao, R. Graf, H. W. Spiess, S. Rastogi, *Macromolecules* **2008**, *41*, 2514.
[22] Y. Yao, R. Graf, H. W. Spiess, S. Rastogi, *Macromol. Rapid Commun.* **2009**, *30*, 1123.
[23] T. Miyoshi, A. Mamun, *Polym. J.* **2012**, *44*, 65.
[24] R. Bärenwald, S. Goerlitz, R. Godehardt, A. Osichow, Q. Tong, M. Krumova, S. Mecking, K. Saalwächter, *Macromolecules* **2014**, *47*, 5163.
[25] R. Kurz, A. Achilles, W. Chen, M. Schäfer, A. Seidlitz, Y. Golitsyn, W. Paul, G.Hempel, J. Kressler, T. Miyoshi, T. Thurn-Albrecht, K. Saalwächter, *Macromolecules* **2017**, *50*, 3890.
[26] N. Kafle, Y. Makita, Y. Zheng, D. Schwarz, H. Kurosu, P. Pan, J. M. Eagan, Y. Nakama, S. Hyano, T. Miyoshi, *Macromolecules* **2021**, *54*, 5705.
[27] S. W. Mowry, G. C. Rutledge, *Macromolecules* **2002**, *35*, 4539.
[28] M. Schäfer, N. Wallstein, M. Schulz, T. Thurn-Albrecht, K. Saalwächter, *Macromol. Chem. Phys.* **2019**, *221*, 1900393.
[29] M. Hikosaka, *Polymer* **1987**, *28*, 1257.
[30] A. Keller, M. Hikosaka, S. Rastogi, A. Toda, P. J. Barham, G. Goldbeck-Wood, *J. Mater. Sci.* **1994**, *29*, 2579.
[31] G. Strobl, *Eur. Phys. J. E* **2000**, *3*, 165.
[32] X. Jiang, G. Reiter, W. B. Hu, *J. Phys. Chem. B* **2016**, *120*, 566.
[33] M. Schulz, A. Seidlitz, R. Kurz, R. Bärenwald, A. Petzold, K. Saalwächter, T. Thurn-Albrecht, *Macromolecules* **2018**, *51*, 8377.
[34] M. Schulz, M. Schäfer, K. Saalwächter, T. Thurn-Albrecht, *Nat. Commun.* **2022**, *13*, 119.
[35] A. Seidlitz, T. Thurn-Albrecht, in *Polymer Morphology: Principles, Characterization, and Processing* (Ed: Q. Guo), John Wiley & Sons, Inc., Hoboken, NJ **2015**, pp. 143–210, Ch. 5.
[36] K. Schäler, A. Achilles, R. Bärenwald, C. Hackel, K. Saalwächter, *Macromolecules* **2013**, *46*, 7818.
[37] M. Schulz, A. Seidlitz, A. Petzold, T. Thurn-Albrecht, *Polymer* **2020**, *196*, 122441.
[38] N. Stribeck, R. G. Alamo, L. Mandelkern, H. G. Zachmann, *Macromolecules* **1995**, *28*, 5029.
[39] N. Stribeck, H. G. Zachmann, R. K. Bayer, F. J. Baltá Calleja, *J. Mater. Sci.* **1997**, *32*, 1639.
[40] A. Toda, *Polymer* **2020**, *211*, 123110.
[41] J.-J. Point, J. Rault, J. D. Hoffman, A. J. Kovacs, L. Mandelkern, B. Wunderlich, E. A. DiMarzio, P. G. de Gennes, J. Klein, R. C. Ball, P. J. Flory, D. Y. Yoon, C. M. Guttman, F. Khoury, I. Voigt-Martin, D. C. Bassett, W. F. X. Frank, E. D. T. Atkins, C. Booth, D. R. Uhlmann, D. T. Grubb, J. H. Magill, D. Vesely, D. M. Sadler, A. Keller, S. Krimm, E. T. Samulski, P. D. Calvert, E. W. Fischer, M. Stamm, et al., *Faraday Discuss. Chem. Soc.* **1979**, *68*, 365.
[42] P. J. Flory, D. Yoon, *Nature* **1978**, *272*, 226.
[43] M. Hikosaka, K. Watanabe, K. Okada, S. Yamazaki, *Adv. Polym. Sci.* **2005**, *191*, 137.
[44] G. Strobl, *The Physics of Polymers: Concepts for Understanding Their Structures and Behavior*, 3rd ed., Springer, Berlin **2007**, pp. XIII, 518 S.
[45] D. R. Lippits, S. Rastogi, G. W. H. Höhne, B. Mezari, P. C. M. M. Magusin, *Macromolecules* **2007**, *40*, 1004.
[46] H. Bu, F. Gu, L. Bao, M. Chen, *Macromolecules* **1998**, *31*, 7108.
[47] C. Bastiaansen, H. Meyer, P. Lemstra, *Polymer* **1990**, *31*, 1435.
[48] F. Christakopoulos, E. Bersenev, S. Grigorian, A. Brem, D. A. Ivanov, T. A. Tervoort, V. Litvinov, *Macromolecules* **2021**, *54*, 5683.
[49] L. Mandelkern, *Acc. Chem. Res.* **1990**, *23*, 380.
[50] E. Robelin-Souffaché, J. Rault, *Macromolecules* **1989**, *22*, 3581.
[51] K. Iwata, *Polymer* **2002**, *43*, 6609.
[52] R. Kurz, M. Schulz, F. Scheliga, Y. Men, A. Seidlitz, T. Thurn-Albrecht, K. Saalwächter, *Macromolecules* **2018**, *51*, 5831.
[53] Y. Men, J. Rieger, G. Strobl, *Phys. Rev. Lett.* **2003**, *91*, 0955026.
[54] R. Graf, A. Heuer, H. W. Spiess, *Phys. Rev. Lett.* **1998**, *80*, 5738.
[55] K. Saalwächter, D. Hinderberger, *ACS Sustainable Chem. Eng.* **2017**, *5*, 11125.
[56] M. Doi, S. F. Edwards, *The Theory of Polymer Dynamics*, Clarendon Press, Oxford **1986**.
[57] C. Luo, J. U. Sommer, *ACS Macro Lett.* **2013**, *2*, 31.

[58] C. Luo, J. U. Sommer, *Phys. Rev. Lett.* **2014**, *112*, 195702.
[59] C. Luo, J. U. Sommer, *ACS Macro Lett.* **2015**, *4*, 30.
[60] C. Luo, M. Kröger, J. U. Sommer, *Macromolecules* **2016**, *49*, 9017.
[61] Y. l. Hong, W. Chen, S. Yuan, J. Kang, T. Miyoshi, *ACS Macro Lett.* **2016**, *5*, 355.
[62] F. Jin, S. Yuan, S. Wang, Y. Zhang, Y. Zheng, Y. l. Hong, T. Miyoshi, *ACS Macro Lett.* **2022**, *11*, 284.
[63] Z. Zhai, C. Fusco, J. Morthomas, M. Perez, O. Lame, *ACS Nano* **2019**, *13*, 11310.
[64] Y. Qin, W. Song, M. Chen, V. Litvinov, Y. Men, *Macromolecules* **2022**, *55*, 5636.
[65] Y. Qiao, M. Schulz, H. Wang, R. Chen, M. Schäfer, T. Thurn-Albrecht, Y. Men, *Polymer* **2020**, *195*, 122425.
[66] Z. Wang, M. Schäfer, A. Petzold, K. Saalwächter, T. Thurn-Albrecht, *Res. Square* **2022**, https://doi.org/10.21203/rs.3.rs-1839187/v1.
[67] B. Heck, G. Strobl, M. Grasruck, *Eur. Phys. J. E* **2003**, *11*, 117.
[68] S. Stepanov, *Phys. Rev. E* **2014**, *90*, 032601.
[69] M. Isobe, W. Krauth, *J. Chem. Phys.* **2015**, *143*, 084509.
[70] L. Zou, W. Zhang, *Macromolecules* **2022**, *55*, 4899.
[71] P. Yi, C. R. Locker, G. C. Rutledge, *Macromolecules* **2013**, *46*, 4723.
[72] M. Anwar, T. Schilling, *Polymer* **2015**, *76*, 307.
[73] T. Shakirov, W. Paul, *Phys. Rev. E* **2018**, *97*, 042501.
[74] T. Shakirov, *Entropy* **2019**, *21*, 856.
[75] P. Panine, V. Urban, P. Boesecke, T. Narayanan, *J. Appl. Cryst.* **2003**, *36*, 991.
[76] W. Janke, W. Paul, *Soft Matter* **2016**, *12*, 642.
[77] T. Shakirov, *Comp. Phys. Commun.* **2018**, *228*, 38.
[78] N. C. Karayiannis, K. Foteinopoulou, C. F. Abrams, M. Laso, *Soft Matter* **2010**, *6*, 2160.
[79] A. Abe, J. Furuya, Z. Zhou, T. Hiejima, Y. Kobayashi, *Adv. Polym. Sci.* **2005**, *181*, 121.
[80] T. Shakirov, W. Paul, *J. Chem. Phys.* **2019**, *150*, 084903.
[81] T. Wu, T. Pfohl, S. Chandran, M. Sommer, G. Reiter, *Macromolecules* **2020**, *53*, 8303.

Kay Saalwöchter completed his chemistry diploma in 1997 at the Institute of Macromolecular Chemistry (University of Freiburg, Germany) and his doctorate in 2000 at the University of Mainz, working with H.W. Spiess at the MPI for Polymer Research. His habilitation followed in 2004 at the University of Freiburg, then becoming a professor of experimental physics at the Martin-Luther-University Halle-Wittenberg (Halle, Germany). His group's research circles around the use and development of a variety of NMR techniques to study structure and dynamics in polymeric, liquid-crystalline, biological, and other "soft" materials, applying also complementary techniques such as rheology, X-ray scattering, and dielectric spectroscopy.

Thomas Thurn-Albrecht is a professor of experimental polymer physics at the Martin Luther University Halle-Wittenberg (Germany). He studied physics at the University of Freiburg (Germany) and Edinburgh University (UK). After completing his Ph.D. with Prof. G. Strobl at the University of Freiburg in 1994, he conducted postdoctoral research at the Max Planck Institute for Polymer Research (Germany) and the University of Massachusetts (USA). His research interests include semicrystalline polymers, polymer crystallization, and structure of semiconducting polymers.

Wolfgang Paul obtained his diploma (in 1986) and Ph.D. (in 1989) at the University of Mainz after studying physics there and at the University of Essen. In 1997, he obtained his habilitation in theoretical physics and became an adjunct professor in Mainz in 2003. Since 2009, he is a full professor of theoretical polymer physics at the University of Halle. His group is mainly working on the computational statistical physics of polymers.